05

Using of ion-beam etching of free-standing films for the development of wavefront correctors in the EUV wavelength range

© N.N. Tsybin, E.B. Kluenkov, A.Ya. Lopatin, V.I. Luchin, A.E. Pestov, N.I. Chkhalo

Institute of Physics of Microstructures, Russian Academy of Sciences,
603950 Nizhny Novgorod, Russia
e-mail: tsybin@ipmras.ru

Received April 26, 2024
Revised April 26, 2024
Accepted April 26, 2024

A method for creating free-standing film elements designed to correct wavefront aberrations in optical systems in the spectral region of the soft X-ray and extreme ultraviolet range has been proposed. Samples of film structures with a uniform transmission across the aperture of at least 60% at a wavelength of 13.5 nm, serving as the initial basis for the formation of phase correctors with a characteristic value of phase modulation corresponding to a change in the optical path length of ~ 1 nm, were manufactured. The possibility of using ion etching to locally change the thickness of free-standing multilayer films has been demonstrated.

Keywords: multilayer free-standing films, wavefront corrector, ion beam etching, soft X-ray and extreme ultraviolet wavelengths.

DOI: 10.61011/TP.2024.07.58798.144-24

Introduction

To achieve the diffraction limit of resolution of the optical scheme (systems of multilayer X-ray mirrors in the soft X-ray (SX) and extreme ultraviolet (EUV) wavelength ranges) it is required to have the wavefront accuracy better than some level usually defined by the Marechal criterion [1]. According to this criterion, the wavefront aberration of the optical system (in terms of a root mean square (RMS) value) shall meet RMS $\leq \lambda/14$, where λ is the operating wavelength. The Marechal criterion is not sufficient any longer for 13.5 nm optical circuits of the projection lithography due to their specific features (partially coherent illumination and stringent requirements for the shape and accuracy of the position of imaged features to be formed on the resist), and the RMS deviation of wavefront shape from the ideal shape shall be $\lambda/50$ [2] — this ensures that residual aberrations will not affect significantly the focus depth and achievable resolution. Thus, requirements for the allowable deviation of the mirror shape in lithography machines are on the subnanometer level with respect to the RMS deviation (0.06 nm for six mirror projection system).

It is a challenging technological task to achieve such high accuracies. And therefore inaccuracies in the working surface profile and relative positioning of mirrors (hereinafter referred to as errors) are almost inevitable and result in permanent or temporary distortion of the wavefront shape. These may be mirror shape errors made in the substrate fabrication process or after depositing a multilayer coating on them (due to internal stresses in the coating). Wavefront distortions may be also caused by variation of individual mirror shapes (due to heating or wrong attachment), inaccurate mirror positioning. Some errors can be successfully removed by means of adjustment of the mirror attachment systems and position or by other available methods (e.g. selective mirror heating [3]), the remaining error may be attempted to be removed using wavefront correctors.

A correction method for local wavefron distortions in an optical system has been proposed earlier and implied removal of a part of reflecting coating of the multilayer mirror by means of ion milling [4,5]. Through removal of a part of reflecting coating (some number of periods), the reflected radiation receives additional phase shift (in case when the real part of refraction index of the multilayer structure on the operating wavelength is $n < 1$), because a part of path will be in vacuum compared with radiation reflected by neighboring areas. When the phase shift is to be reduced, then the mirror coating thickness may be increase locally (at $n < 1$) by sputtering additional periods above the coating. Such approach is used to make a local change in the phase distribution of the radiation front reflected from the multilayer coating with the distribution over amplitude remaining unchanged. The latter is satisfied when the initial number of periods in the multilayer coating is quite high such that the reflectance is weakly dependent on the number [5], and, consequently, the removal of some number of periods almost does not affect the reflecting properties of the coating. Thus, the method is effective, if the constant low wavefront distortion in the optical system is to be corrected. However, it has some disadvantages associated with the requirement to remove a coated mirror to perform correction (local ion milling or additional sputtering) and replace it again. Moreover, additional difficulties may be associated with the protecting layer that is used on the mirror coatings and affects the degree of phase shift. This cap layer is first to be removed in the place of correction, and then to be applied again.

A more simple and convenient method of wavefront correction that does not require removing the mirror — is to add a transmissive corrector in the form of a free-standing film with nonuniform thickness to the optical system [6]. Two options of the film corrector may be available consisting of one or two individual film structures that define the desired phase shift pattern („phase“ part — PP) and compensate the intensity distribution variation appearing after the „phase“ part radiation transmission („amplitude“ part — AP). Since there are no transparent materials in the SX and EUV wavelength range radiation passing through the film corrector will be absorbed, which is a disadvantage of this correction method. To minimize absorption in the film corrector, most transparent materials shall be used on the operating wavelength and the film corrector thickness shall be minimized.

Brittleness of free-standing thin films is another disadvantage of film correctors. Since generally the thicker the free-standing film the stronger it is, then PP and AP shall be preferably combined in a single structure to make film correctors with high transmittance. In this case, it is also unnecessary to orient accurately PP and AP of the film corrector relative to each other.

Free-standing films with uniform thickness are used in many SX and EUV spectral range applications as absorption spectral filters, polarizers and transmissive phase shifters, protective films for a mask in EUV projection lithography systems [7–10]. However, the film corrector is a film with nonuniform thickness. To achieve the desired material distribution over the free-standing film aperture, a film with the required thickness distribution may be applied to the substrate as early as at the film deposition stage (using, for example, shaped diaphragms installed above the magnetrons). Also, a corrector workpiece (free-standing film) with uniform thickness may be prepared initially, and the desired thickness distribution may be achieved by local removal of a part of free-standing film material, for example, using ion beam etching. The first approach is more simple to use if the film shall be thickened in some places, while ion etching is used to achieve local film thinning more easily. It is expected that these approaches will be combined in future for film corrector fabrication. Potential applications of ion-beam etching for local thinning (uniform or gradient) of film corrector workpieces will be addressed herein.

1. Choosing film corrector materials

Materials for corrector PP and AP shall be chosen both according to the optical constants on the operating wavelength and to suitability of these material for film corrector fabrication. Film corrector options for a wavelength of 13.5 nm are discussed herein. Wavelength choice is determined by the fact that the diffraction quality optics is primarily used in EUV lithography systems. Applications of both traditional — using a reflective mask, and maskless projection lithography on 13.5 nm are currently addressed [11]. In case when a shorter wavelength (most promising options are those with operating wavelengths of 6.6 or 11.2 nm [12]) EUV lithography development program is launched in Russia, then there will be little difficulty in transferring this approach to these wavelengths.

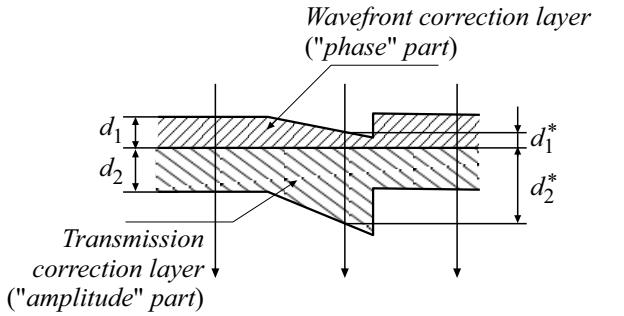

Figure 1. Schematic diagram of the film wavefront corrector for the SX and EUV wavelength range with linear dependence of phase shift on position and with transparency aligned with respect to the aperture

Consider a two-layer film corrector with a linear thickness gradient (both in PP and in AP for intensity adjustment) (Figure 1).

Optical path difference Δ_{12} corresponding to phase shift on a particular wavelength between the „phase“ and „amplitude“ part areas with different thicknesses can be calculated knowing the optical constants of materials:

$$\Delta_{12} = \Delta - \Delta^* = (1 - n_1) \cdot d_1 + (1 - n_2)d_2 - (1 - n_1)d_1^* - (1 - n_2)d_2^* \approx (1 - n_1) \cdot (d_1 - d_1^*). \quad (1)$$

„*“ herein denotes the quantities associated with the beam passing through the film corrector in the area where layer thicknesses differ from the initial ones (Figure 1). Expression (1) neglected two terms because it is obvious that AP shall have real part of the refraction index close to 1 ($n_2 \approx 1$) to prevent any phase distortions. Considering that the reflectance in the EUV wavelength band with normal incidence from the layer is low, it can be shown that the maximum transmittance of the two-layer corrector for the set phase shift is calculated by the following expression:

$$T_{\max} = \exp(-\Delta_{12} \cdot 4\pi/\lambda \cdot 1/[(1 - n_1)/k_1 - (1 - n_2)/k_2]), \quad (2)$$

where n_1, n_2, k_1, k_2 are real and imaginary parts of the refraction index.

The maximum transmittance (with set phase shift) corresponds to the case when there is only PP in one place and only AP in the neighboring area, which is obviously impracticable. In other words, the maximum transmittance of the film corrector will be inherently lower than $T_{\max}$. But the equation can be used to choose the best materials for the two-layer corrector. It is clear that the highest transmittance of the corrector is achieved when $[(1 - n_1)/k_1 - (1 - n_2)/k_2]$ is maximum.

Table 1. Values of the real part n and imaginary part k of the refraction index and $(1-n)/k$ for some materials on 13.5 nm [13]

Material	n	k	$(1-n)/k$
Si	0.999	0.00183	0.546
B_4C	0.96	0.00572	6.993
SiC	0.982	0.00481	3.742
Mo	0.924	0.00645	11.783
Nb	0.932	0.0053	12.830
Zr	0.959	0.00377	10.875
Ru	0.887	0.017	6.647
$MoSi_2$	0.969	0.00434	7.143
$NbSi_2$	0.971	0.0038	7.632
$ZrSi_2$	0.979	0.00321	6.542

Table 2. Maximum transmittances on 13.5 nm and corresponding (minimum) thicknesses of PP and AP layers in two-layer film correctors that can theoretically provide the phase shift corresponding to the path difference of 1 nm calculated using equations (2) and (3) and data from Table 1

Pair of materials (1st−2nd)	T_{max},%	d_1^{min}, nm	d_2^{min}, nm
Nb−Si	92.7	15.36	44.48
Mo−Si	92.05	13.8	48.63
Zr−Si	91.38	25.68	52.9
Mo−$ZrSi_2$	83.73	29.6	59.5
Zr−$ZrSi_2$	80.67	61.2	71.9

Table 1 shows the values of the real part n and the imaginary part k of the refraction index on 13.5 nm and $(1-n)/k$ taken from [13] for the most widely used film materials that have a relatively low absorption coefficient on 13.5 nm.

The table shows that Si shall be used as AP on 13.5 nm, and Nb−Si shall be used as a pair that provides the maximum transmission with the desired phase shift. Knowing the desired phase shift, minimum material thicknesses can be also calculated:

$$d_2^{min} \cdot k_2 = d_1^{min} \cdot k_1 = \Delta_{12}/[(1-n_1)/k_1 - (1-n_2)/k_2]. \quad (3)$$

Examples of parameter calculations for some pairs that provide phase shift corresponding to a path difference of 1 nm are shown in Table 2.

Certainly, when choosing film corrector materials, fabricability of films with this composition, stress-strain properties, oxidation resistance and possibly heat resistance shall be also considered (the latter is important in case when more powerful radiation will pass through the film corrector). Since multilayer structures may have a higher strength than multilayer structures [14], multilayer structures (consisting of alternating pairs of nanometer-thick layers) may be used as film corrector workpieces. Another advantage of multilayer structures is in that internal stresses in the film may be changed (reduced), if required, through choosing the layer composition and thickness. Higher internal stresses in the film are undesirable because they can result in film twisting when it is separated from the substrate or even to film damage (when the ultimate strength is exceeded). Film corrector workpiece samples that have only multilayer PP or both multilayer PP and AP are shown herein.

2. Research methods

Free-standing multilayer film structures with uniform thickness (film corrector workpieces) were fabricated using our previously developed technique [8]. A sublayer (layer Y) and multilayer corrector structure were deposited on the polished Si wafers of 100 mm in diameter by the magnetron sputtering method. In some cases, a supporting polymer layer of about 100 nm in thickness was applied additionally to the surface of the multilayer structure deposited on the substrate. The polymer layer was used for additional hardening of the film to avoid film damage when it is separated from the substrate. The polymer layer was removed at the last stage by immersing the samples in toluene or through ultraviolet photodestruction of polymer components in air during several hours (mercury-vapor lamps were used). When making the free-standing structure, the sublayer was solved in a selective etch (hydrochloric acid water solution), and the film separated from the substrate was placed onto polished stainless steel rings or Si frames with a hole up to 80 mm in diameter (Figure. 2).

Films stretched on a frame were also made for the experiments. For this, the free-standing film caught onto the Si frame was stretched by adding adhesive on the inside perimeter of the frame ring (on the film boundary). Then, frames coated with epoxy adhesive were bonded to the

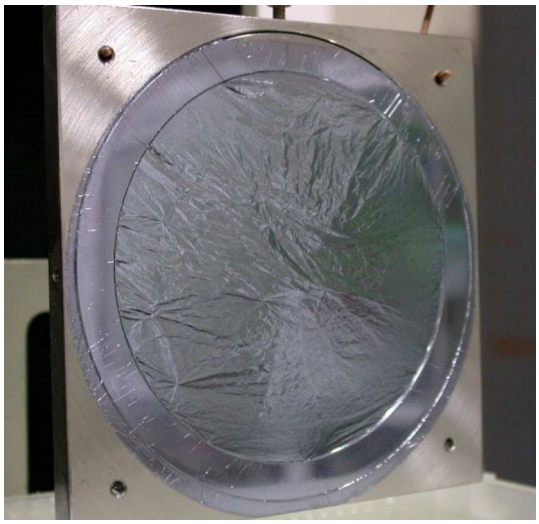

Figure 2. (Zr-3 nm/$ZrSi_2$-1.5 nm)×10+ (Si-2.5 nm/$ZrSi_2$-0.7 nm) × 20 film corrector workpiece caught onto the Si frame with a 80 mm hole secured in the holder, with the applied hardening polymer layer.

stretched film until the contact was achieved. The stretched film is more resistant to external impacts and therefore there are better chances to avoid damage when the sample is placed in the vacuum volume and air is evacuated from the volume for ion etching.

Then the corrector workpieces were placed into an ion-beam etching system. The system described in detail in [15] is equipped with a sample stage and KLAN-103M (NTK „Platar“) wide-aperture accelerated ion source. Argon was used as the working gas. The ion-optical system of the source with outlet aperture in the form of an ellipse with semi-axes 90 and 60 mm ensures quasi-parallel (divergence max.$\pm 3^\circ$) monoenergetic (energy spread ± 4 eV) ion beam.

The size of the sample area exposed to the ion beam was limited by the diaphragm placed in front of the sample. A damper could be placed additionally on a motor-driven linear translator in front of the diaphragm. By moving the damper when the sample was exposed to the ion beam, a nonuniform etching depth profile along the damper movement direction could be achieved.

To determine the etching rate of the PP or AP corrector materials, structures with the same period were deposited onto the Si substrates and the material was sputtered under the beam through the diaphragm that cut out a part of the incident beam on the sample. The depth of removal (step height on the ion beam exposure boundary) was defined depending on time by the measurements using the Talysurf CCI 2000 optical profilometer.

The corrector workpiece transmittance was measured using the laboratory bench [16]. Operating principle of the bench is described below. Image of the „point“ EUV source (demountable X-ray tube with Si target, Si L_α-line radiation, wavelength 13.5 nm) is transferred to the test sample by spherical and flat multilayer Nb/Si mirrors. The radiation transmitted through the film sample is recorded by the detector — FDUK-100UV Si photodiode. The sample stage (carousel) is motor-driven and makes it possible to perform scanning along the sample surface at 0.3 mm intervals. The beam width at half maximum is about 0.65 mm. The relative measurement accuracy of the transmittance was 0.1%.

3. Results

The first experiments with ion-beam etching of stretched films have demonstrated that ripple occurs after removal of a part of material from the surface of the stretched film (Figure 3). Such behavior may be caused by local heating and/or internal stress variation in the exposure area. Unidirectional folding might be caused by initial nonuniform film stretching. nevertheless, since the film transmittance near the normal weakly depends on the angle of incidence and the phase shift, due to the smallness of $(1 - n)$, varies slowly as the thickness increases , folding does not have any significant effect on the amplitude and phase of the transmitted radiation. For example, in case of shallow folds with a typical size of about 100 μm and peak to valley value of about 5 μm, addition to the optical path difference of 1 nm will be about 0.005 nm, and the transmittance reduction will be about 0.15% when transmittance of an unfolded phase corrector is 60%.

At the first stage, the material was removed uniformly by the ion beam (ion current $I_{ion} = 10$ mA, accelerating voltage $U_{acc} = 500$ V) in the sample center (through a square diaphragm) and the sample transmittance was measured using the laboratory reflectometer with normal incidence on 13.5 nm (Figure 4). The entire Si layer of about 75 nm in thickness was removed at the specified parameters of the ion beam during t = 15 min. The transmittance curve shows that there is a shelf in the exposure area indicating good uniformity of the ion beam and uniform removal. Note that when scanning the sample placed on the test bench carousel , the beam successively passed through the hole outside the sample (transmittance T = 1), sample frame (T = 0), sample itself, frame (T = 0) again and exited to the hole outside the sample again, therefore, the signal shape shown in the figure is observed.

At the next stage, at attempt was made to create a linear sample thickness gradient by using the uniformly moving damper. The damper opened gradually the square hole in the diaphragm through which an ion beam entered the sample. Figure 5 shows the photographs of $Zr/ZrSi_2$- and $Nb/ZrSi_2$ structures with Si „amplitude“ part, with a linear Si thickness gradient in the center, and the transmittance measurement on the aperture of one of the samples on 13.5 nm.

The curve of the intensity recorded by the detector vs. the coordinate along the sample aperture consists of several typical areas. A zero intensity of the transmitted signal is observed initially when the beam enters the supporting frame, then a sharply rising front (whose profile is defined by the final width of the probing beam), horizontal plateau corresponding to the unetched part of the film and then the transmittance growth area can be seen, which corresponds to the ion-beam etched area. Smooth drop observed on the boundary of the maximum removed material is associated with the fact that the diaphragm forming the beam on the sample is at a finite distance from the sample (several millimeters) and, therefore, a film area near the boundary is exposed to ions on a shadow side.

The curve (Figure 5) shows that a near-linear intensity gradient of radiation transmitted through the film has been formed successfully.

Conclusion

SX and EUV diffraction optical systems may use phase correctors to remove wavefront errors induced by X-ray mirror positioning and surface shape inaccuracies. One of the possible options is the transmissive film corrector placed additionally into the optical system.

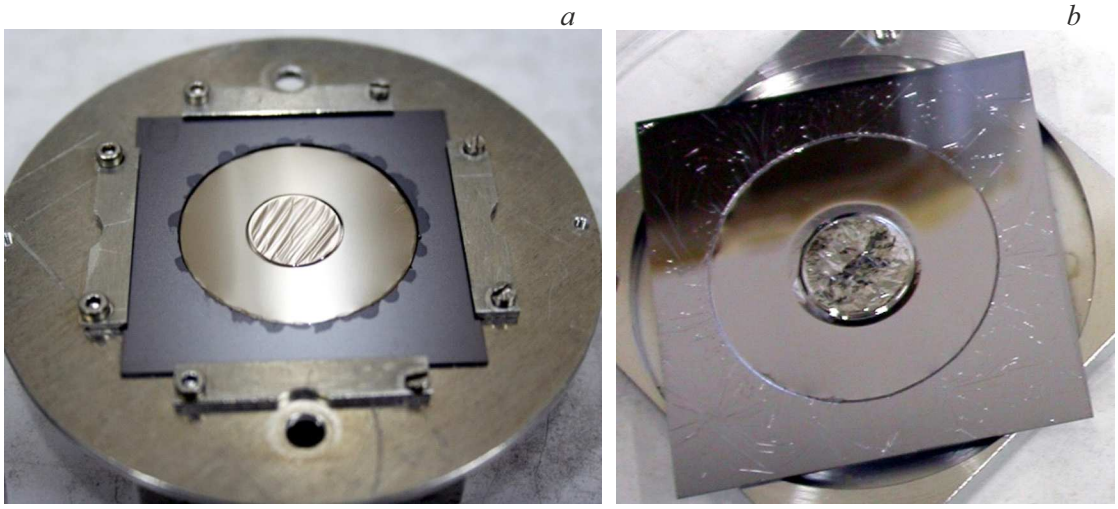

Figure 3. Photographs of free-standing stretched films, Ø 30 mm, uniformly etched in the center. *a* — (Zr-3 nm/$ZrSi_2$-1.5 nm) × 10+ Si-75 nm structure etched during $t = 12$ min, at ion current $I_{ion} = 10$ mA, accelerating voltage $U_{acc} = 500$ V from the Zr/$ZrSi_2$ side. Thickness of the etched off part is about 20 nm, etched side is shown; *b* — (Zr-3 nm/$ZrSi_2$-1.5 nm) × 10 + (Si-5 nm/$ZrSi_2$-1.5 nm) × 12 film sample etched on the Si/$ZrSi_2$ side.

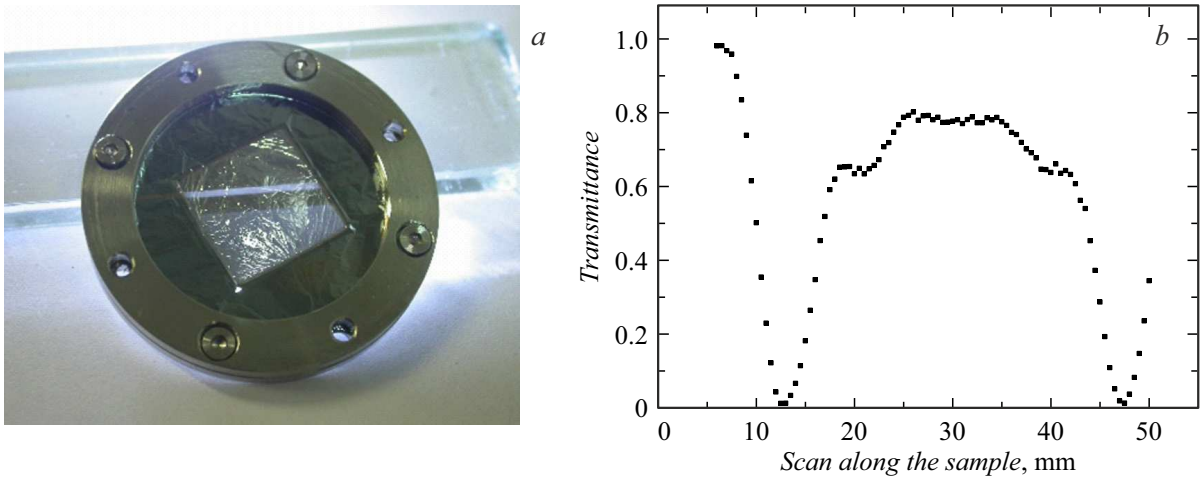

Figure 4. *a* — photograph of (Zr-3 nm/$ZrSi_2$-1.5 nm) × 10 + Si-75 nm sample after ion-beam etching during $t = 15$ min through a square hole on the Si side; *b* — dependence of the sample transmittance on 13.5 nm on the position.

The study describes the fundamental principles for choosing the film corrector materials to ensure the highest transmittance with the desired phase shift.

Film corrector workpieces (films with uniform thickness) with an aperture up to 80 mm and transmittance of at least 60% on the operating wavelength of 13.5 nm were fabricated. The workpieces consist of two parts: the „phase“ part having a refraction index not equal to 1 that is used for phase correction of the transmitted radiation, and the „amplitude“ part having a refraction index close to 1 that is designed to compensate the intensity distribution variation after radiation transmission through the „phase“ part. To increase the strength, the phase and/or amplitude parts of the correctors were made in the form of multilayer films.

The workpieces were used for experiments to create film thickness distributions by removing a part of film under ion beam exposure. The applicability of ion-beam etching was demonstrated for uniform removal of a part of film or formation of a linear thickness gradient, which indicates the benefits of such approach.

Funding

The study was supported financially by the Ministry of Science and Higher Education, agreement No. 075-15-2021-1350 dated October 5, 2021 (reference number 15.SiN.21.0004).

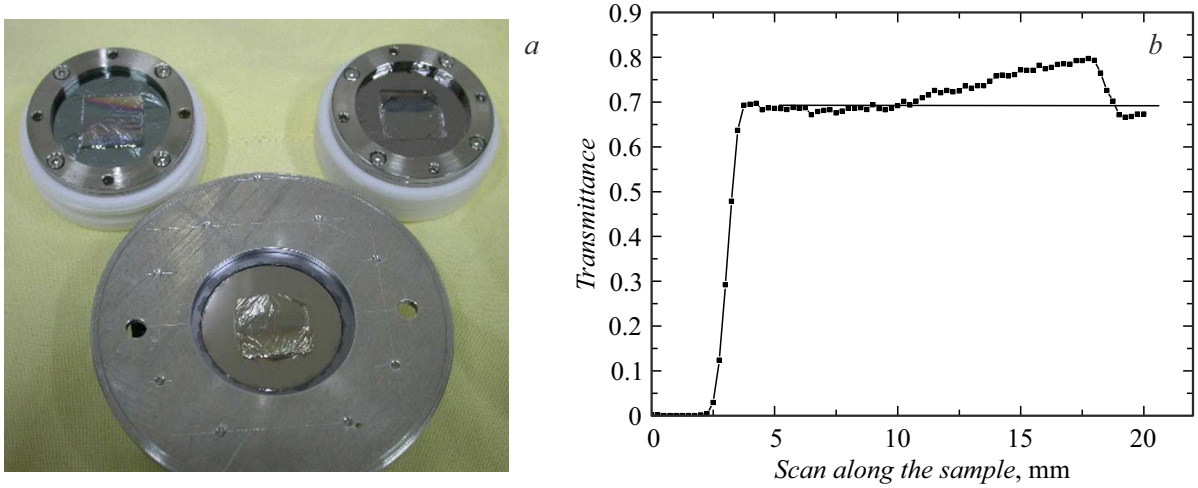

Figure 5. *a* — photograph of film corrector workpieces, Ø 30 mm, with linear film thickness gradient; *b* — transmittance measurement on 13.5 nm of (Nb-3 nm/$ZrSi_2$-1.5 nm) × 7+ Si-80 nm structure etched on the Si side with linear gradient ion-beam etching time (process variables: $U_{acc} = 500$ V, $I_{ion} = 10$ mA, $t = 15$ min).

Conflict of interest

The authors declare that they have no conflict of interest.

References

[1] M. Born, E. Volf. *Osnovy optiki* (Nauka, M., 1973) (in Russian)
[2] V. Bakshi. *EUV Lithography* (SPIE, John Wiley & Sons, Inc., 2008)
[3] R. Saathof, G.J.M. Schutten, J.W. Spronck, R.H.M. Schmidt. Precision Engineer., **41**, 102 (2015). DOI: 10.1016/j.precisioneng.2015.03.004
[4] M. Singh, M.F. Bal, J.J.M. Braat, D. Joyeux, U. Dinger. Appl. Opt., **42** (10), 1847 (2003). DOI:10.1364/ao.42.001847
[5] M. Yamamoto. Nucl. Instrum. Methods A, **467–468** (2), 1282 (2001). DOI: 10.1016/S0168-9002(01)00640-4
[6] B. Bittner, N. Wabra, S. Schneider et al. Patent DE102012202057B4. 10.02.2012.
[7] N.I. Chkhalo, M.N. Drozdov, S.A. Gusev, E.B. Kluenkov, A.Ya. Lopatin, V.I. Luchin, N.N. Salashchenko, L.A. Shmaenok, N.N. Tsybin, B.A. Volodin. Proc. SPIE, **8076**, 80760O-1 (2011). DOI: 10.1117/12.886781
[8] N.I. Chkhalo, M.N. Drozdov, E.B. Kluenkov, A.Ya. Lopatin, V.I. Luchin, N.N. Salashchenko, N.N. Tsybin, L.A. Sjmaenok, V.E. Banine, A.M. Yakunin. J. Micro/Nanolith. MEMS MOEMS., **11** (2), 021115 (2012). DOI: 10.1117/1.JMM.11.2.021115
[9] S.Yu. Zuev, A.Ya. Lopatin, V.I. Luchin, N.N. Salashchenko, N.N. Tsybin, N.I. Chkhalo. Russ. Microelectron., **52** (5), 354 (2023) (in Russian). DOI: 10.31857/S0544126923700539
[10] A.D. Akhsakhalyan, E.B. Kluenkov, A.Ya. Lopatin, V.I. Luchin, A.N. Nechay, A.E. Pestov, V.N. Polkovnikov, N.N. Salashchenko, M.V. Svechnikov, M.N. Toropov, N.N. Tsybin, N.I. Chkhalo, A.V. Shcherbakov. J. Surf. Investigation: X-ray, Synchrotron and Neutron Techniques, **11** (1), 1 (2017). DOI:10.1134/S1027451017010049
[11] N.N. Salashchenko, N.I. Chkhalo, N.A. Dyuzhev. Poverkhnost. Rentgen. sinkhrotr. i neitron. issled. **10**, 10 (2018). (in Russian). DOI: 10.1134/S0207352818100165
[12] N.I. Chkhalo, N.N. Salashchenko. AIP Advances, **3**, 082130 (2013). DOI: 10.1063/1.4820354
[13] Electronic source. Available at: https://cxro.lbl.gov/
[14] M.S. Bibishkin, N.I. Chkhalo, S.A. Gusev, E.B. Kluenkov, A.Y. Lopatin, V.I. Luchin, A.E. Pestov, N.N. Salashchenko, L.A. Shmaenok, N.N. Tsybin, S.Y. Zuev. Proc. SPIE, **7025**, 702502 (2008). DOI:10.1117/12.802347
[15] N.I. Chkhalo, E.B. Kluenkov, A.E. Pestov, V.N. Polkovnikov, D.G. Raskin, N.N. Salashchenko, L.A. Suslov, M.N. Toropov. Nucl. Instrum. Methods Phys. Res. A, **603** (1–2), 62 (2009). DOI: 10.1016/j.nima.2008.12.160
[16] M.S. Bibishkin, I.G. Zabrodin, I.A. Kas'kov, E.B. Kluenkov, A.E. Pestov, N.N. Salashchenko, D.P. Tchekhonadskikh, N.I. Chkhalo, L.A. Shmaenok. Izvestiya AN. Ser. fiz., **68** (4), 560 (2004) (in Russian).

Translated by E.Ilinskaya